Journal of Inflammation Research Dovepress

Open Access Full Text Article ORIGINAL RESEARCH

Integrated Data Mining and Animal Experiments to Investigate the Efficacy and Potential Pharmacological Mechanism of a Traditional Tibetan Functional Food *Terminalia chebula Retz*. in Hyperuricemia

Wenbin Liu[1,2,*], Mingchao Zhang[3,*], Jingli Tan[1,2], Hao Liu[1,2], Lijun Wang[1,2], Jingyang Liao[1,2], Dan Huang[1,2], Wang Jie[1,2], Xiaobao Jin[1,2]

[1]School of Basic Medical Sciences, Guangdong Pharmaceutical University, Guangzhou, People's Republic of China; [2]Guangdong Provincial Key Laboratory of Pharmaceutical Bioactive Substances, Guangdong Pharmaceutical University, Guangzhou, People's Republic of China; [3]People's Hospital of Foshan Nanhai Economy Development Zone, Foshan, People's Republic of China

*These authors contributed equally to this work

Correspondence: Xiaobao Jin; Wang Jie, Guangdong Provincial Key Laboratory of Pharmaceutical Bioactive Substances, GuangDong Pharmaceutical University, Guangzhou, Guangdong, 510006, People's Republic of China, Tel +861 358 056 5879, Fax +86020-3935 2184, Email jinxf2001@163.com; wangjie19870122@163.com

Background: Hyperuricemia (HUA), a common metabolic disorder associated with gout, renal dysfunction, and systemic inflammation, necessitates safer and more comprehensive therapeutic approaches. Traditional Tibetan medicine has a rich history of treating HUA. This study aimed to identify novel anti-hyperuricemic herb derived from traditional Tibetan medicine.

Methods: Traditional Tibetan medicine prescriptions for HUA were analyzed using data mining techniques, identifying *T. chebula* as a high-frequency herb. Its phytochemical composition was characterized by UPLC-QE-Orbitrap-MS. Hyperuricemic rat models were treated with *T. chebula* to assess its effects on serum uric acid (UA) levels, renal inflammation, intestinal barrier integrity, and gut microbiota composition. Molecular and histological analyses evaluated its impact on key biomarkers.

Results: Through data mining, we identified *T. chebula* as a promising candidate for HUA treatment. *T. chebula* demonstrated dose-dependent inhibition of xanthine oxidase (XOD) in vitro and significantly reduced serum UA levels and XOD activity in vivo. It restored gut barrier function by upregulating tight junction proteins (ZO-1, Occludin, Claudin-1) and reduced pro-inflammatory cytokines (IL-6, TNF-α). *T. chebula* improved renal function, reducing serum creatinine (Cre) and blood urea nitrogen (BUN) levels. Gut microbiota analysis revealed a favorable shift in microbial composition, with reductions in harmful bacteria (eg, *Clostridium* spp.) and increases in beneficial bacteria (eg, *Roseburia*). These effects aligned with the modulation of the gut-kidney axis.

Conclusion: This study highlights the multi-target therapeutic potential of *T. chebula* in HUA management. By regulating the gut-kidney axis, *T. chebula* alleviates systemic inflammation, enhances intestinal and renal health, and addresses critical aspects of HUA pathology. These findings underscore the value of integrating traditional medicine with modern scientific methodologies to develop innovative treatments.

Keywords: *Terminalia chebula Retz*., hyperuricemia, intestinal flora, renal, data mining

Introduction

Hyperuricemia (HUA), a prevalent metabolic disorder, is a growing health concern in China owing to its association with a range of serious conditions. HUA can be caused by excessive uric acid production or insufficient renal and intestinal excretion. It is not only a risk factor for gout but is also closely associated with the onset and progression of conditions

Received: 24 September 2024
Accepted: 5 December 2024
Published: 17 December 2024

Graphical Abstract

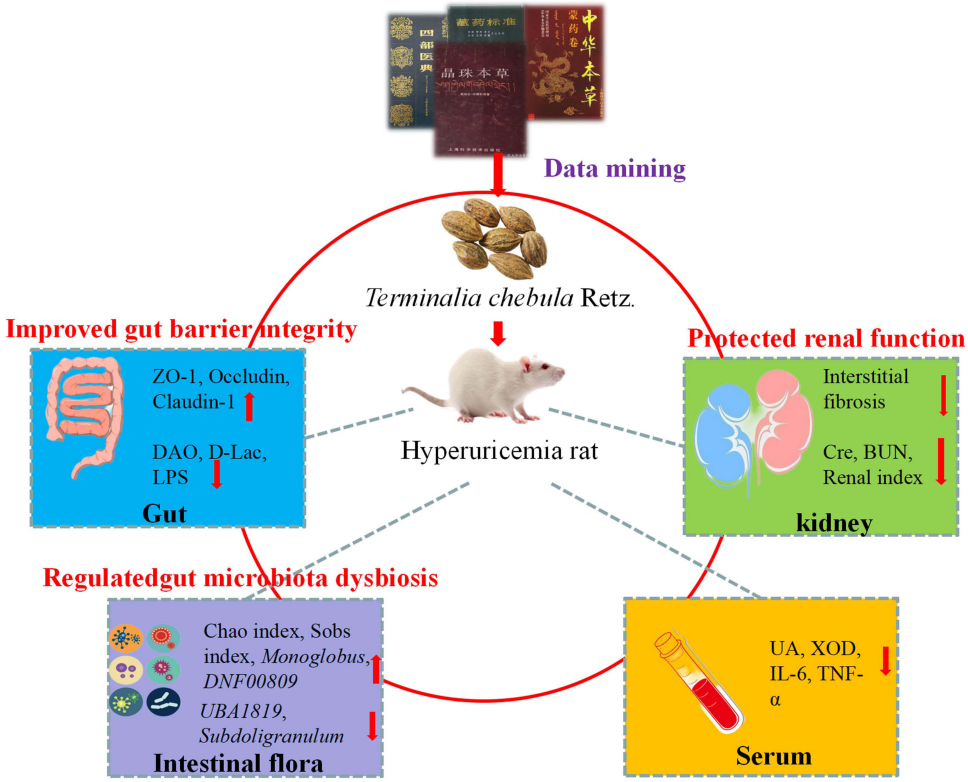

such as hypertension, diabetes, and kidney disease. Epidemiological studies have revealed a steady increase (by as much as 17.4%) in the prevalence of HUA in China.[1] It is currently the second most common metabolic disorder, occurring only in patients with diabetes. Moreover, the affected population is becoming progressively younger, which is expected to place a significant burden on China's healthcare system in the coming years. The general strategy for HUA primarily focuses on the use of xanthine oxidase (XOD) inhibitors, such as allopurinol and febuxostat, to lower uric acid levels, and the use of uricosuric agents, such as probenecid, benzbromarone, and sulfinpyrazone, to promote uric acid excretion. However, adverse reactions associated with XOD inhibitors and uricosuric agents, including diarrhea, headache, rash, severe allergies, and nephrotoxicity, often limit their clinical use. Furthermore, these treatments focus narrowly on serum uric acid reduction, failing to address other critical aspects of HUA pathology, such as renal protection and gut microbiota modulation. This underscores the pressing need for safer and more holistic therapeutic approaches.[2]

Recent studies highlight the crucial role of the gut-kidney axis in uric acid metabolism and HUA pathology. The gut influences systemic uric acid levels by degrading purines, producing short-chain fatty acids, and maintaining intestinal barrier integrity. Meanwhile, the kidneys, responsible for the majority of uric acid excretion, share closely linked inflammatory and metabolic pathways with the gut. Dysregulation of this axis can exacerbate HUA and associated complications. Recognizing its importance, researchers are increasingly exploring treatments for HUA by targeting the gut-kidney axis. For instance, the Cichorium intybus L. formula has been shown to regulate gut microbiota dysbiosis and provide renal protection in HUA nephropathy rats.[3] Similarly, the traditional Chinese medicine (TCM) formula CoTOL demonstrated uric acid reduction, potentially through its regulation of intestinal flora.[4] These findings highlight the therapeutic potential of targeting gut-kidney interactions.

Tibet is a high-altitude region characterized by elevated atmospheric pressure and low air density. The Tibetan population predominantly leads a nomadic lifestyle with dietary preferences for beef, barley, and butter tea. Nearly 50%

of Tibetan adults consume alcohol. The incidence of HUA in the Tibetan region is significantly higher than in other parts of China, with a crude prevalence rate as high as 37.2%. Traditional Tibetan medicine, with its unique theoretical framework, is an essential component of traditional Chinese medicine. Over the years a wealth of traditional prescriptions for the treatment of HUA have been utilized.[5] For example, RuPeng 15 powder,[6] Shi Wei Ru Xiang powder,[7] and TongFeng Tangsan[8,9] have been widely used in Tibetan hospitals to treat HUA and their efficacy confirmed by clinical studies.

This study initially screened Tibetan medical prescriptions for HUA treatment described in classical Tibetan medical books. Through data mining, *T. chebula* was identified as a potential candidate anti-HUA medication. It is worth noting that no existing literature has reported on the use of *T. chebula* extract for the treatment of HUA. Subsequently, the therapeutic effects of *T. chebula* were validated by establishing a HUA rat model, and the potential mechanisms of action were explored. This study serves as a theoretical reference for understanding the biological functions of *T. chebula* and its application in HUA treatment.

Materials and Methods

Data Mining of Tibetan Medicine Prescriptions for the Treatment of HUA

To systematically analyze and quantify traditional Tibetan medicine knowledge, extensive data mining of prescriptions for hyperuricemia (HUA) treatment was conducted. Key sources included the *National Standard for Tibetan Medicine, rGyud-bzhi, Crystal Beads Materia Medica, Chinese Tibetan Medicine*, and *Chinese Materia Medica-Tibetan Medicine*. Using the keyword "huangshui", historically associated with HUA, relevant prescriptions were identified and extracted. These prescriptions were digitized and structured into a comprehensive dataset using Microsoft Excel. The data were standardized based on the 2020 edition of the Chinese Pharmacopoeia to ensure consistency and comparability. Unlike traditional qualitative interpretations, we used modern data-driven methods to uncover patterns and relationships within the dataset. The frequency of each Tibetan medicine was calculated using Excel pivot tables, transforming the dataset into a transactional format suitable for advanced analysis. Subsequently, we imported this data into IBM SPSS Modeler 18.0 for co-occurrence analysis, enabling us to explore patterns of simultaneous use among Tibetan medicines. Finally, to gain deeper insights, we performed hierarchical cluster analysis using IBM SPSS Statistics 20.[10]

T. chebula Extract Preparation

T. chebula fruits were sourced from Lincang, Yunnan, China, and identified by Professor Ma Hongyan (School of Traditional Chinese Medicine, Guangdong Pharmaceutical University). A voucher specimen (GDPUHTC01) is stored in the Herbarium of the Guangdong Provincial Key Laboratory of Pharmaceutical Bioactive Substances. The fruits were dried at 60 °C, ground into powder, and extracted three times by reflux with distilled water (ddH_2O) for 0.5 hours per cycle. The extracts were concentrated under vacuum at 60 °C to remove the solvent.

Qualitative Analysis of T. chebula by UPLC-QE-Orbitrap-MS

Qualitative analysis of *T. chebula* was performed using ultra-high-performance liquid chromatography (UPLC) coupled with a Q Exactive Orbitrap mass spectrometer (Thermo Fisher Scientific, USA). Chromatographic separation was achieved on a Thermo Gold C18 column (1.7 μm, 2.1×100 mm) at 40 °C, with a mobile phase comprising 0.1% formic acid in water (A) and methanol (B). The gradient elution program was as follows: 0–5.0 min, 20% B; 5.0–45.0 min, 20–100% B; 45.0–56.1 min, 20–100% B; and 56.1–60.0 min, 20% B.

The mass spectrometric analysis employed an electrospray ionization (ESI) source in both positive and negative modes with a mass range of m/z 200–1000. The resolution was set to 35,000 (primary) and 17,500 (secondary). Key operational parameters included a spray voltage of 3500 V, capillary temperature of 320 °C, probe heater temperature of 350 °C, sheath gas flow rate of 35 units, auxiliary gas flow rate of 10 units, and collision energies of 20, 25, and 30 eV.

Animal Experiments

36 SPF-grade male Sprague-Dawley rats (180 and 220.0 g) were obtained from Guangdong Medical Laboratory Animal Center (Certificate number: 44007200101564). After a one-week acclimatization period, rats were randomly divided into six groups (n = 6/group): Control, Model, allopurinol (ALLO, positive control, GKH Pharmaceutical Ltd., lot: H44021695), and high-dose (HZHI), middle-dose (HZME), and low-dose (HZLO) *T. chebula* groups. Following the method described by Yang et al,[11] all groups except the Control group were administered 10% fructose solution via oral gavage from weeks 1 to 6. Through preliminary experiments, we determined the dosing regimen for *T. chebula*. To induce the HUA rat model, potassium oxonate solution (600 $mg \cdot kg^{-1}$) was also orally administered from weeks 2 to 6. During this period, the Control and Model groups received an equivalent volume of 0.5% CMC-Na solution, the ALLO group received allopurinol solution (50 $mg \cdot kg^{-1}$), and the HZLO, HZME, and HZHI groups were given *T. chebula* solutions at doses of 45 $mg \cdot kg^{-1}$, 90 $mg \cdot kg^{-1}$, and 180 $mg \cdot kg^{-1}$, respectively, for 4 weeks.

Histopathological Examination and Immunohistochemistry (IHC)

Kidney and intestine tissues were fixed in 4% paraformaldehyde, dehydrated, embedded in paraffin, and sectioned at 4 μm. For histological analysis, sections were stained with hematoxylin and eosin (H&E) or Masson's trichrome stain. Immunohistochemistry (IHC) was used to assess the expression of Claudin-1, Occludin, and ZO-1. Stained sections were examined under a light microscope (Olympus, Tokyo, Japan), and the percentage of positively stained areas was quantified using ImageJ software.

Biochemical Detection/ Plasma Biochemical Assay

Serum was obtained by centrifuging blood at 3800 rpm for 10 min at 4 °C. Serum levels of uric acid (UA), blood urea nitrogen (BUN), creatinine (Cre), and xanthine oxidase (XOD) activity were measured using commercial assay kits (Jiancheng Bioengineering Institute, Nanjing, China). Enzyme-linked immunosorbent assay (ELISA) kits (Jiangsu Meimian Industrial Co., Ltd., Yancheng, China) were used to quantify lipopolysaccharide (LPS), TNF-α, IL-6, diamine oxidase (DAO), and D-lactate (D-Lac).

RNA Extraction, Reverse-Transcription, and Quantitative PCR

Total RNA from intestinal tissues was extracted using an RNA extraction kit (Vazyme Biotech Co., Ltd., Nanjing, China) following the manufacturer's protocol. RNA concentration was measured with a micro-spectrophotometer (Allsheng Biotech Co., Ltd., Hangzhou, China), and cDNA was synthesized using a two-step RT-qPCR kit (Seven Biotech Co., Ltd., Beijing, China). Gene expression levels of Claudin-1, Occludin, and ZO-1 were analyzed on a real-time PCR system, with β-Actin as the internal control. The RT–PCR protocol included 95 °C for 30s, followed by 40 cycles of 95 °C for 30s and 60 °C for 30s. Gene expression was calculated using the $2^{-\Delta\Delta Ct}$ method. Primer sequences are listed in Table 1.

Table 1 Primer Sequences of RT-qPCR

Gene	Primer	Sequence (5'to3')
Occludin-1	Forward	TCTCTCAGCCGGCATACTCT
	Reversed	GCGATGCACATCACGATGAC
ZO-1	Forward	ACAGCCAGCTCTTGGTCATC
	Reversed	GTATGGTGGCTGCTCAAGGT
Claudin-1	Forward	TGGCATGAAGTGCATGAGGT
	Reversed	CCCAGCCAGTAAAGAGAGCC
β-actin	Forward	AGGGAAATCGTGCGTGACAT
	Reversed	GAACCGCTCATTGCCGATAG

Intestinal Microbiota Analysis

On the final day of the experiment, fecal samples were collected from each rat group and stored at −80 °C. The samples were sent to Shanghai Meiji Biological Technology Co., Ltd. (Shanghai, China) for intestinal microbiota analysis. The V3–V4 region of 16S rDNA was amplified using universal primers (338F: ACTCCTACGGGAGGCAGCA; 806R: GGACTACHVGGGTWTCTAAT). Amplified DNA fragments were purified with an Axygen DNA Gel Recovery Kit (Axygen Inc., Massachusetts, USA) and used to construct an Illumina library with the TruSeq™ DNA Sample Prep Kit (Illumina Inc., San Diego, CA, USA). Sequencing was performed on the Illumina MiSeq™ System to obtain microbiota sequencing data.

Statistical Analysis

Data are presented as mean ± standard deviation (SD). Statistical analyses were conducted using GraphPad Prism (version 8.0.1). One-way ANOVA was employed to analyze differences among multiple groups, followed by Tukey's HSD (Honestly Significant Difference) test as the post hoc method to identify significant pairwise group differences. A p-value < 0.05 was considered statistically significant.

Results

Data Mining of Tibetan Medicine Prescriptions for the Treatment of HUA

From various sources, we retrieved 122 prescriptions aimed at treating HUA, including the National Standard for *Tibetan Medicine, rGyud-bzhi, Crystal Materia Medica, Chinese Tibetan Medicine*, and *Chinese Materia Medica-Tibetan Medicine* (Tables S1 and S2). These prescriptions included 248 herbal drugs. Unlike traditional qualitative descriptions, we applied modern data mining techniques to analyze and quantify the use of these herbs systematically. Using frequency analysis, we identified the most commonly used Chinese medicines for HUA treatment, including *T. chebula, Juemingzi, Ruxiang, Shexiang, Muxiang, Doukou, Huangkuizi, Maohezi, Shuichangpu*, and *Yuganzi* (Figure 1A). Notably, *T. chebula* emerged as the most frequently cited species, occurring 54 times and accounting for 44.3% of those identified. Furthermore, co-occurrence analysis revealed that *T. chebula* exhibited the highest co-occurrence rates with Muxiang (n=26), Maohezi (n=20), Shuichangpu (n=19), Juemingzi (n=22), Yuganzi (n=19), Ruxiang (n=21), Huangkuizi (n=18), and Shexiang (n=21) (Figure 1B). These analyses not only validated *T. chebula*'s central role in traditional prescriptions but also uncovered potential synergistic relationships with co-occurring herbs, which are not explicitly documented in historical texts. The configuration of different Tibetan medicine combinations was determined using the hierarchical clustering method, which classifies herbs based on their relationships with other Tibetan medicines. In our study, this hierarchical clustering process resulted in the stratification of Tibetan medicines into three distinct and effective prescriptions (Figure 1C). To validate the potential therapeutic value of the most frequently prescribed medicine for HUA, *T. chebula*, we conducted in vitro assays to assess its inhibitory activity against XOD. The results demonstrated that *T. chebula* exhibited a dose-dependent reduction in XOD activity, further supporting its use as a promising candidate for HUA treatment (Figure 1D).

Qualitative Analysis of Phytochemical Constituents in T. chebula

UPLC-QE-Orbitrap-MS was used to identify the major phytochemical constituents of *T. chebula*. The total ion chromatograms (TICs) of *T. chebula* are shown in Figure 2A and B, and their chemical structures are shown in Figure 2C. Through high-resolution UPLC-MS/MS analysis, 47 constituents were rapidly identified from *T. chebula* based on their accurate MS and MS/MS data, together with comparisons with references (Table S3). These constituents included phenols, terpenoids, flavonoids, sulfonamides, fatty acids, glucosides, and steroids (Figure S1).

T. chebula Decreased UA Level in Hyperuricemic Rats

To further validate the potential therapeutic value of *T. chebula* in HUA, we induced a rat HUA model using fructose-water and potassium oxonate (Figure 3A). As shown in Figure 3B, the body weight of all rats increased steadily throughout the experimental period, with no significant differences observed among the six groups. In the third week, the

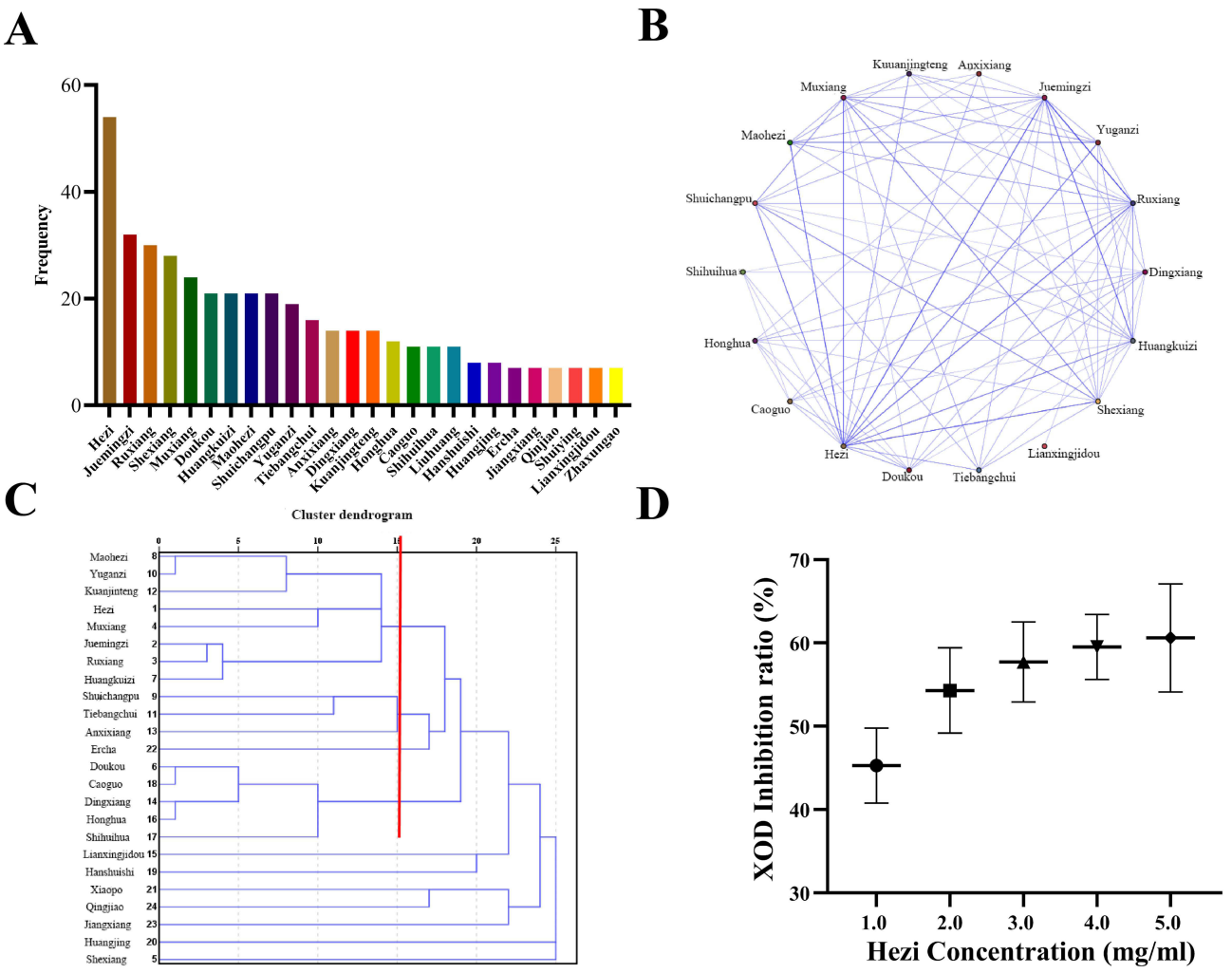

Figure 1 Data mining of Tibetan medicine prescriptions in the treatment of UA. (**A**) High-frequency Chinese medicines in prescriptions. (**B**) Herbs co-occurrence diagram. (**C**) Hierarchical cluster analysis of herbs. (**D**) The inhibitory activity of *T. chebula* on XOD in vitro.

serum UA level of the model group was approximately three times higher than that of the normal group, a statistically significant difference as determined by Tukey's HSD post hoc test ($P < 0.01$). This result confirms the successful establishment of the HUA rat model. After 4 weeks of treatment, both *T. chebula* and allopurinol significantly reduced serum UA levels and XOD activity compared with those in the model group (UA: $P = 0.000$, $P = 0.000$, $P = 0.000$, all $P < 0.01$, Tukey's HSD; XOD: $P = 0.003$, $P = 0.005$, $P = 0.004$, all $P < 0.01$, Tukey's HSD) (Figure 3C and D). In clinical practice, HUA is often accompanied by an inflammatory response. Elevated serum UA levels can trigger the release of pro-inflammatory cytokines, thereby increasing the risk of renal inflammation and injury. In our study, serum proinflammatory cytokines IL-6 and TNF-α were significantly increased in HUA rats compared to those in normal rats (IL-6: $P = 0.000$, $P < 0.01$, Tukey's HSD; TNF-α: $P = 0.006$, $P < 0.01$, Tukey's HSD). Notably, *T. chebula* significantly restored IL-6 and TNF-α levels (IL-6: $P = 0.000$, $P = 0.004$, $P = 0.001$, all $P < 0.01$, Tukey's HSD; TNF-α: $P = 0.006$, $P = 0.012$, $P = 0.012$, $P < 0.01$ or $P < 0.05$, Tukey's HSD) (Figure 3E and F).

T. chebula Protected Renal Function of Hyperuricemic Rats

Numerous studies have documented the potential of HUA to induce renal dysfunction and pathological alterations in the kidney, thereby posing a considerable threat to patient well-being. The kidney plays an indispensable role in the regulation of uric acid balance. Figure 4A presents the results of the H&E and Masson staining of kidney sections derived from the six groups of experimental rats. In the control group, the kidney morphology exhibited a normal

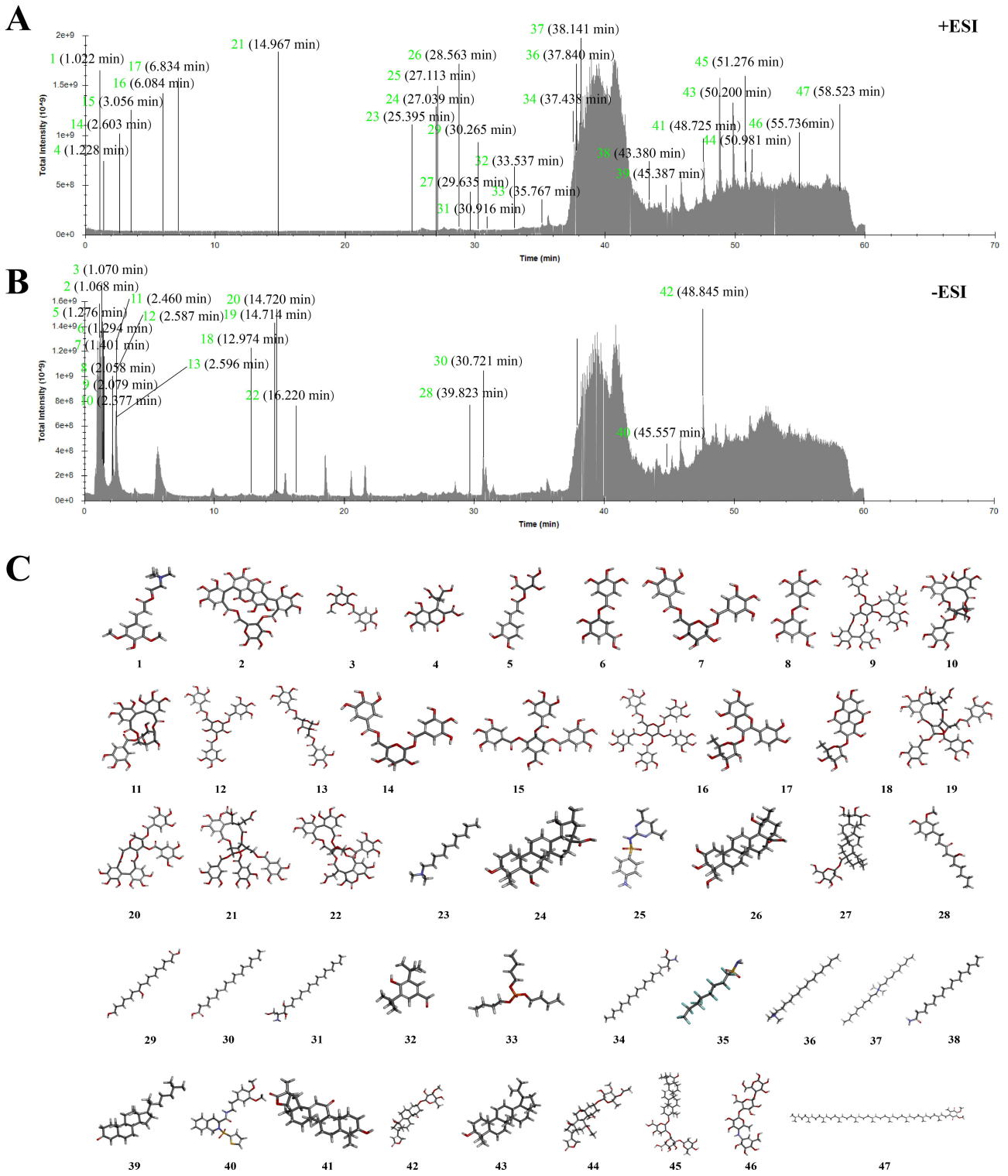

Figure 2 Chemical composition analysis and identification of *T. chebula*. (**A**) Total ion chromatograms of *T. chebula* extract in positive mode. (**B**) Total ion chromatograms of *T. chebula* extract in negative mode. (**C**) The structure of the chemical composition identified in *T. chebula*..

appearance without any histopathological deviations. Conversely, HUA rats displayed noticeable dilation of the tubular lumen and observable infiltration of inflammatory cells within the kidney tissue. Masson's staining revealed banded interstitial fibrosis along with a proliferation of collagen fibers. Remarkably, *T. chebula* administration at varying doses resulted in kidney morphology that closely resembled that of the normal control group. Moreover, there was a significant

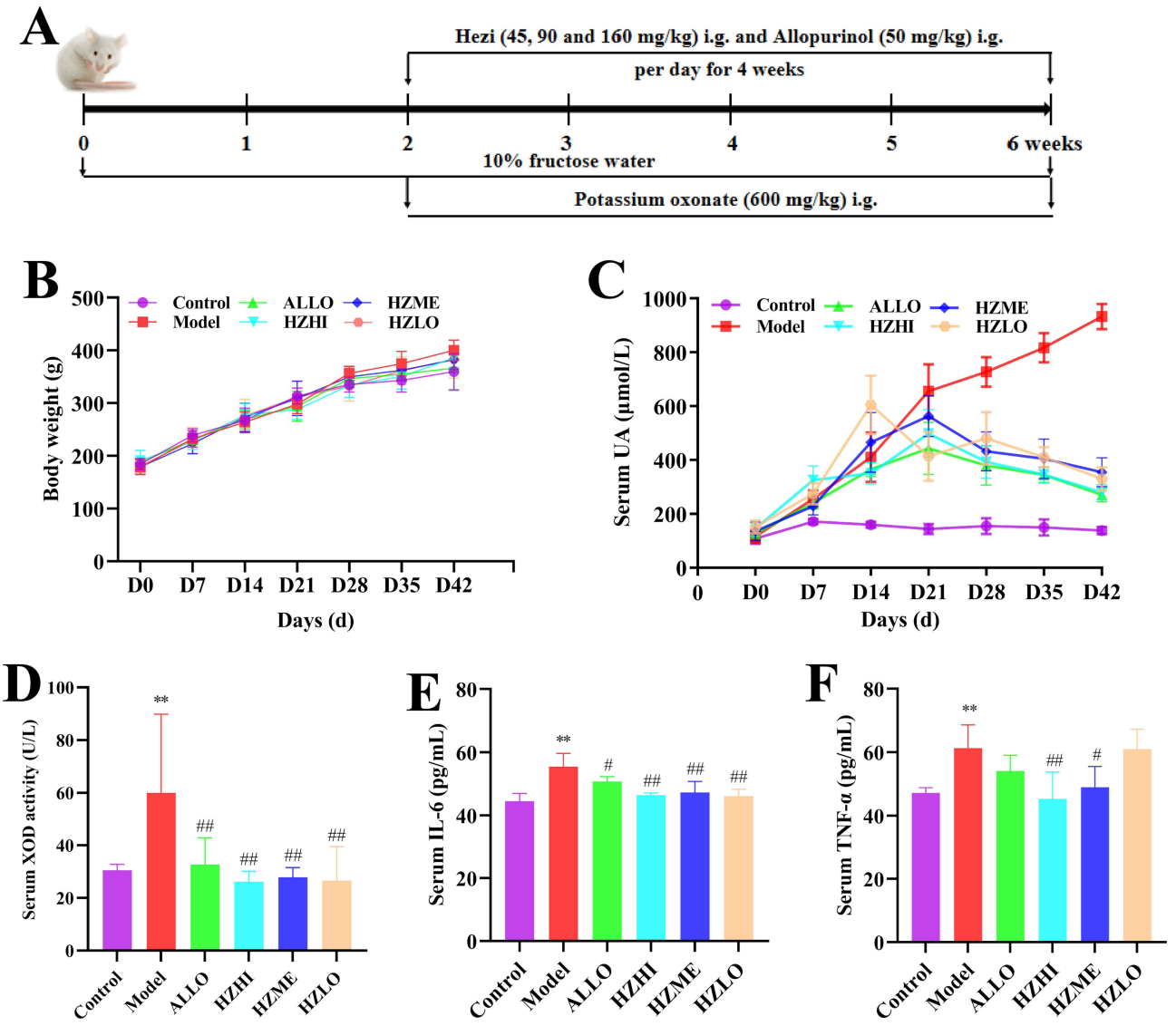

Figure 3 The therapeutic effects of *T. chebula* on HUA rats. (**A**) Schematic experimental design for *T. chebula* treatment. (**B**) Body weight. (**C**) Serum UA. (**D**) Serum XOD activity. (**E**) Serum IL-6. (**F**) Serum TNF-α. Values are presented as mean ± SD (n = 6 per group). Statistical significance was assessed using one-way ANOVA followed by Tukey's HSD test. $^{**}P < 0.05$ vs Control group; $^{\#}P < 0.05$, $^{\#\#}P < 0.05$ vs Model group.

reduction in banded interstitial fibrosis, which implies the effective mitigation of histopathological kidney damage in HUA rats. Figure 4B–4D illustrate the renal index, serum BUN, and Cre levels across all experimental groups. After 42 days of HUA induction, a substantial increase in the renal index, serum BUN, and Cre levels was observed in the model group compared to that in the control group (Renal index: $P = 0.001$, $P < 0.01$; BUN: $P = 0.000$, $P < 0.01$; Cre: $P = 0.000$, $P < 0.01$, Tukey's HSD). However, subsequent treatment with *T. chebula* extract at various concentrations led to a significant reduction in the renal index, serum BUN, and Cre levels compared to those in the model group (Renal index: $P = 0.000$, $P = 0.000$, $P = 0.000$, all $P < 0.01$, Tukey's HSD; BUN: $P = 0.000$, $P = 0.000$, $P = 0.000$, all $P < 0.01$, Tukey's HSD; Cre: $P = 0.000$, $P = 0.000$, $P = 0.001$, all $P < 0.01$, Tukey's HSD). These findings provide compelling evidence of the effectiveness of *T. chebula* extract in mitigating renal damage induced by HUA.

T. chebula Improved Intestinal Barrier Integrity in Hyperuricemic Rats

The intestine plays a vital role in uric acid excretion. Histological examination using hematoxylin and eosin (HE) staining revealed that high-purine diets and excessive serum uric acid (UA) levels disrupted gut morphology, resulting in

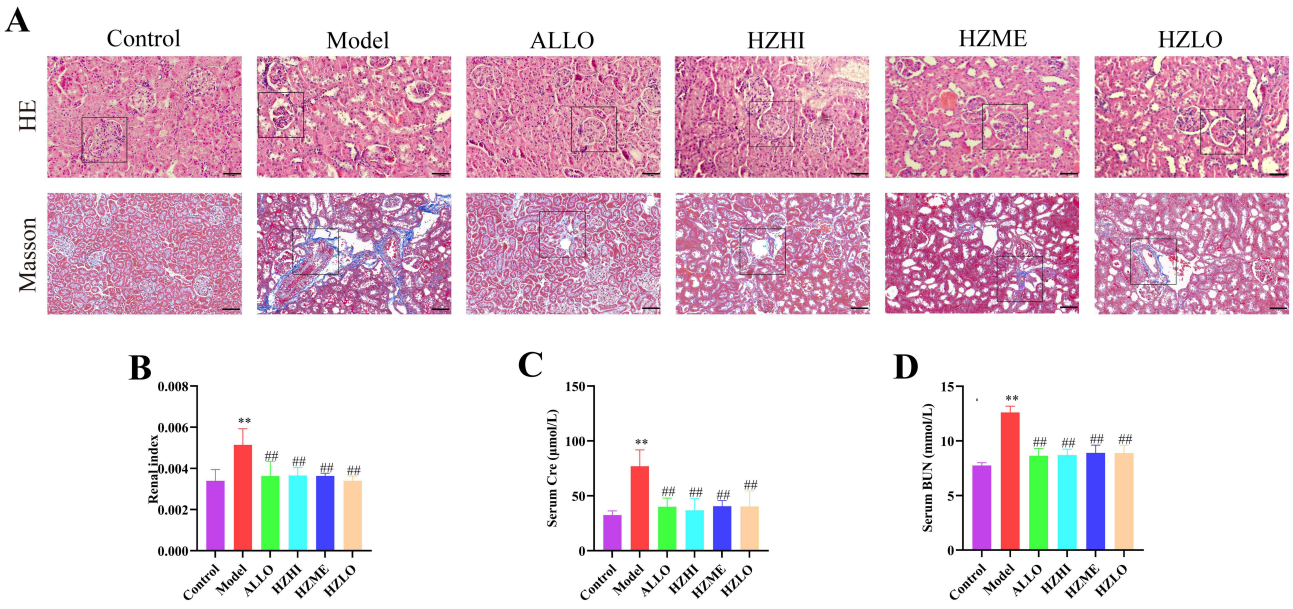

Figure 4 *T. chebula* protected renal function of hyperuricemic rats. (**A**) H&E staining and Masson staining of kidney tissue (blue denotes collagen fibers, bar = 50 μm). (**B**) Renal index. (**C**) Serum Cre. (**D**) Serum BUN. Values are presented as mean ± SD (n = 6 per group). Statistical significance was assessed using one-way ANOVA followed by Tukey's HSD test. $^{**}P < 0.05$ vs Control group; $^{\#\#}P < 0.05$ vs Model group.

shortened villi, villus shedding, and reduced crypt depth. Conversely, treatment with *T. chebula* effectively reversed these morphological changes, as demonstrated by improved villus length and crypt depth ratio (Figure 5A). Serum levels of D-Lac, DAO, and LPS were used as markers to assess gut permeability. As depicted in Figure 5B-5D, in comparison to the control group, the model group showed a significant increase in the serum levels of D-Lac, DAO, and LPS (D-Lac: P =0.000, $P < 0.01$; DAO: P =0.000, $P < 0.01$; LPS: P =0.000, $P < 0.01$, Tukey's HSD). Notably, in the HZHI, HEME, and HZLO groups, the levels of these markers were significantly reduced compared with those in the model group (D-Lac: P =0.000, 0.000, 0.000, all $P < 0.01$, Tukey's HSD; DAO: P =0.000, 0.000, 0.001, all $P < 0.01$, Tukey's HSD; LPS: P =0.000, 0.000, 0.000, all $P < 0.01$, Tukey's HSD). These findings suggest that *T. chebula* effectively repairs gut mucosal damage and enhances intestinal barrier permeability.

Intestinal tight junctions play a crucial role in maintaining the gut barrier function and intestinal homeostasis. The results of the immunohistochemistry experiments showed that the expression levels of ZO-1, Occludin, and Claudin-1, which are proteins associated with intestinal tight junctions, were significantly reduced in the model group (ZO-1: P =0.037, $P < 0.05$; Occludin: P =0.000, $P < 0.01$; Claudin-1: P =0.009, $P < 0.01$, Tukey's HSD). However, treatment with *T. chebula* significantly upregulated the expression of these proteins (ZO-1: P =0.006, 0.003, 0.005, all $P < 0.01$, Tukey's HSD; Occludin: P =0.001, 0.017, $P < 0.01$ or $P < 0.05$, Tukey's HSD; Claudin-1: P =0.004, 0.019, 0.018, $P < 0.01$ or $P < 0.05$, Tukey's HSD) (Figure 6A), indicating that *T. chebula* can effectively maintain gut barrier function. Notably, allopurinol treatment did not affect the expression of these proteins. Consistent with the immunohistochemistry results, *T. chebula* treatment significantly upregulated the mRNA expression of ZO-1, Occludin, and Claudin-1 (ZO-1: P =0.000, 0.000, $P < 0.01$, Tukey's HSD; Occludin: P =0.000 0.000, $P < 0.01$, Tukey's HSD; Claudin-1: P =0.003, 0.002, $P < 0.01$, Tukey's HSD) (Figure 6B and C). Collectively, these findings suggest that *T. chebula* treatment preserves gut barrier function by enhancing tight junction protein expression.

T. chebula Regulated UA-Induced Gut Microbiota Dysbiosis in Hyperuricemic Rats

To assess the impact of *T. chebula* on the intestinal flora of HUA mice, we conducted a comprehensive analysis of gut microbial communities by sequencing the V3-V4 regions of the 16S rRNA gene. Our α-diversity analysis revealed no significant differences in the Shannon and Simpson indices (measures of diversity) among the control, model, and HZHI groups (Figure 7C and D). However, the Chao index and Sobs index (markers of richness) showed a reduction in the

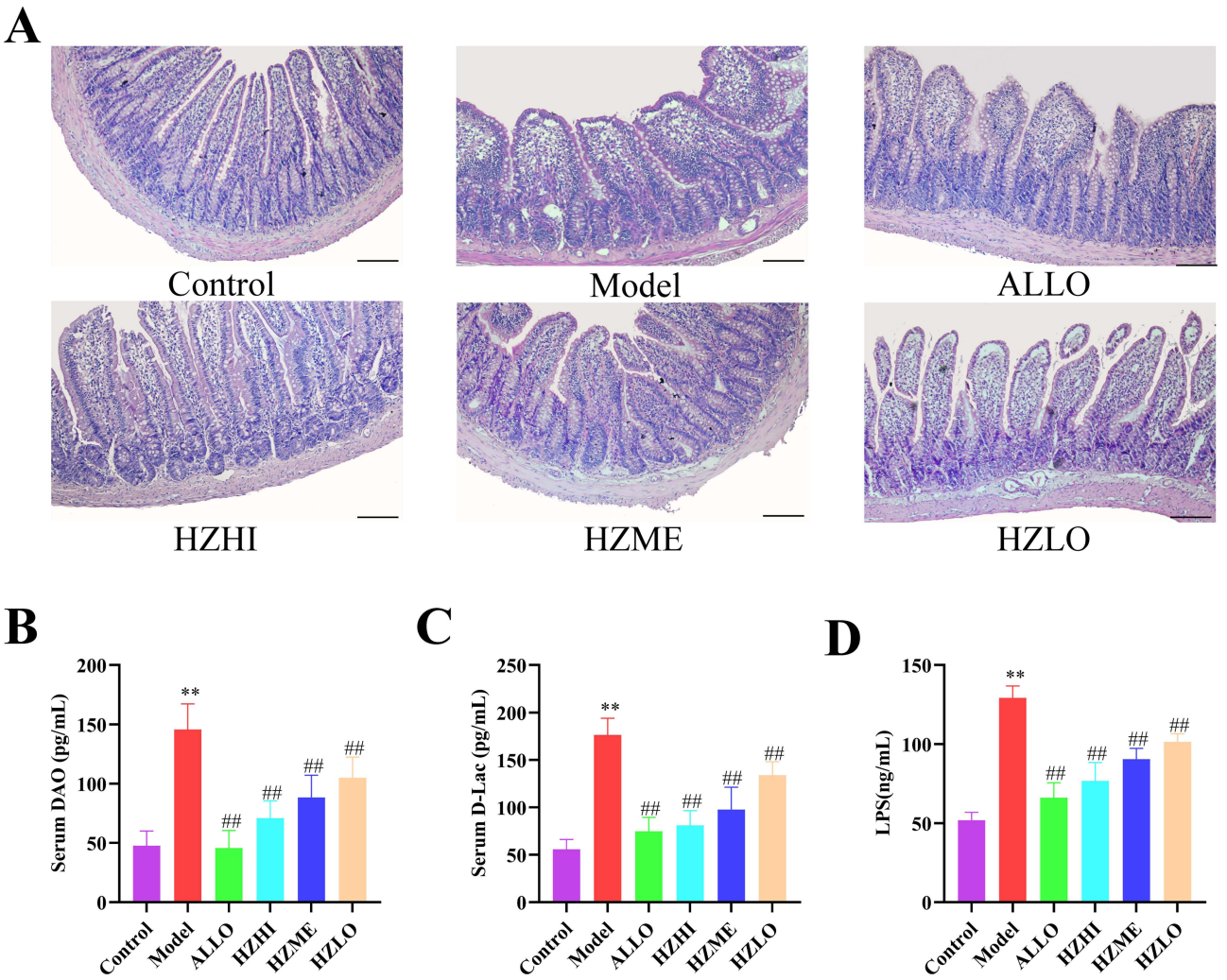

Figure 5 *T. chebula* improved intestinal barrier integrity in hyperuricemic rats (**A**) H&E staining of gut (bar = 100 μm). (**B**) Serum DAO. (**C**) Serum D-Lac. (**D**) Serum LPS. Values are presented as mean ± SD (n = 6 per group). Statistical significance was assessed using one-way ANOVA followed by Tukey's HSD test. $^{**}P < 0.05$ vs Control group; $^{\#\#}P < 0.05$ vs Model group.

model group compared with the control group, whereas the HZHI group exhibited a notable increase in both the Chao index and Sobs index (P =0.034, P =0.008, $P < 0.05$, Tukey's HSD) (Figure 7A and B). At the phylum level, the dominant microbiota primarily consisted of *Firmicutes, Bacteroidetes, Actinobacteria, Patescibacteria, Desulfobacteria*, and *Cyanobacteria* (Figure 8A). At the genus level, the microbiota was predominantly composed of *Romboutsia, Clostridium_sensu_stricto_1, norank_f_Ruminococcaceae, Candidatus_Stoquefichus, Lactobacillus*, and *norank_f_Muribaculaceae* (Figure 8B). Importantly, substantial differences were observed in the species composition at both the genus and phylum levels. Compared to the model group, the HZHI group showed significantly reduced *Actinobacteriota* and *Bacteroidota* levels and elevated *Firmicutes* levels (Figure 7E–H). In summary, these findings demonstrate that *T. chebula* effectively alters the composition and structure of microbiota in HUA rats.

To explore the relationship between alterations in gut microbiota and HUA remission, Spearman correlation analysis was employed to investigate the associations between bacteria and HUA-related metabolic variables at the genus level. The results revealed that *Clostridium_innocuum_group, Clostridium_sensu_stricto_1, Erysipelatoclostridium, Subdoligranulum, Megamonas, Faecalitalea*, and *UBA1819* were positively associated with UA, XOD, IL-6, TNF-α, BUN, Cre, DAO, and D-LAC but negatively correlated with ZO-1, Claudin-1, and Occludin protein levels. In contrast, *Monoglobus, DNF00809*, and *Roseburia* were inversely correlated (Figure 9A). Furthermore, *T. chebula* treatment led to significant reductions in the levels of *Clostridium_innocuum_group, Erysipelatoclostridium, UBA1819,*

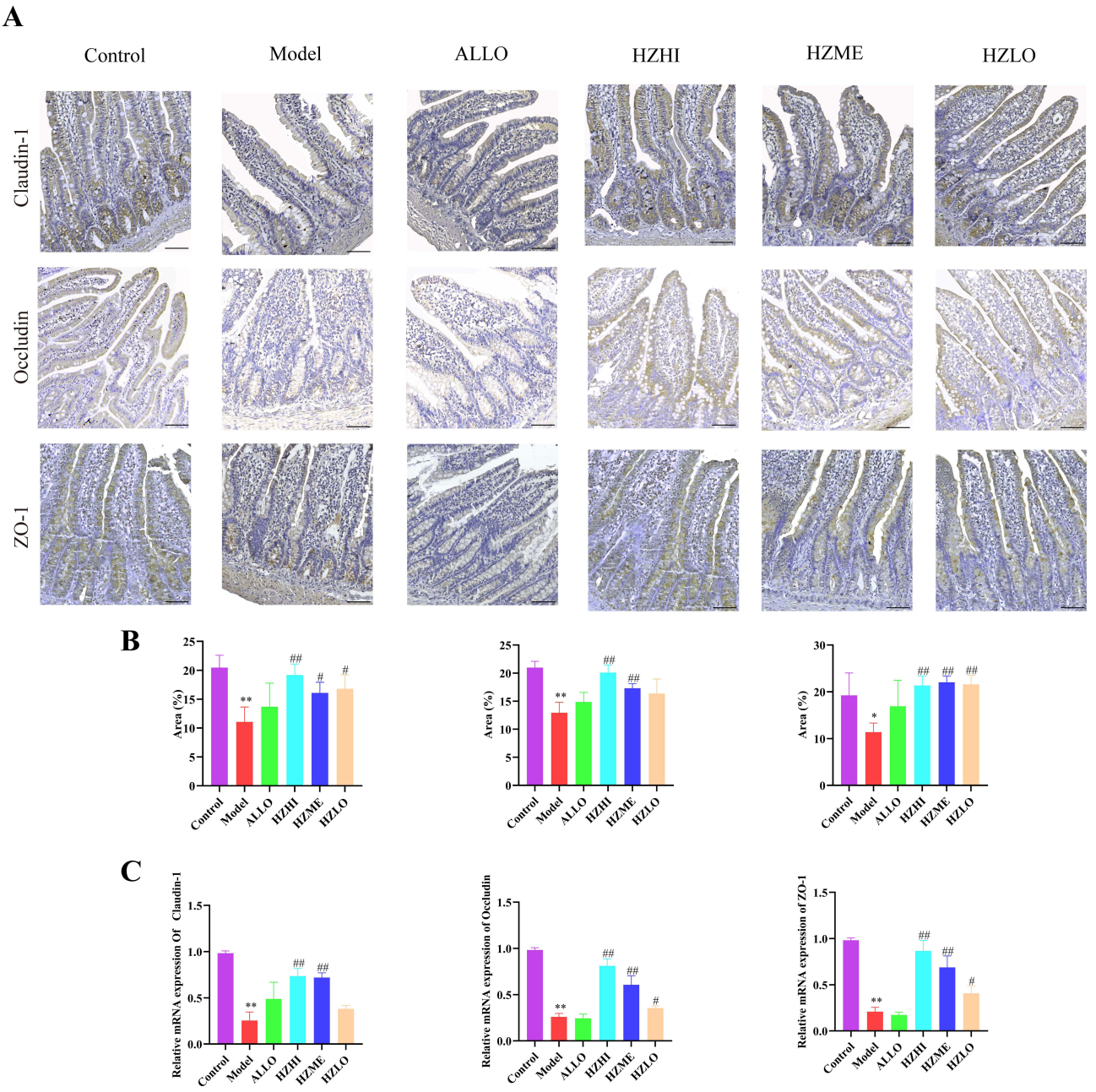

Figure 6 *T. chebula* improved tight junction proteins expression in intestinal. (**A**) ZO-1, Occludin, and Claudin-1 immunohistochemical staining in intestinal (bar = 50 μm). (**B**) Statistical analysis of the percentage of the ZO-1, Occludin, and Claudin-1 positively stained area. (**C**) ZO-1, Occludin, and Claudin-1 mRNA expression by RT-PCR. Values are presented as mean ± SD (n = 6 per group). Statistical significance was assessed using one-way ANOVA followed by Tukey's HSD test. **P*< 0.05, ***P*< 0.05 vs Control group; $^{\#}P < 0.05$, $^{\#\#}P < 0.05$ vs Model group.

Subdoligranulum, and *Clostridium_sensu_stricto_1* (P =0.009, P =0.047, P =0.042, P =0.010, P =0.012, $P < 0.01$ or $P < 0.05$, Tukey's HSD) (Figure 9B–F) and significant increases in the levels of *Monoglobus, DNF00809*, and *Roseburia* in the model group (P =0.049, P =0.000, P =0.042, $P < 0.01$ or $P < 0.05$, Tukey's HSD) (Figure 9G–I). These findings provide valuable insights into the potential of *T. chebula* treatment to induce HUA remission by affecting the composition of gut microbiota.

Discussion

Owing to changes in modern lifestyles, the prevalence of HUA has been steadily increasing every year, making it the second most common metabolic disorder after diabetes.[12] Hence, there is an urgent need to develop new anti-HUA

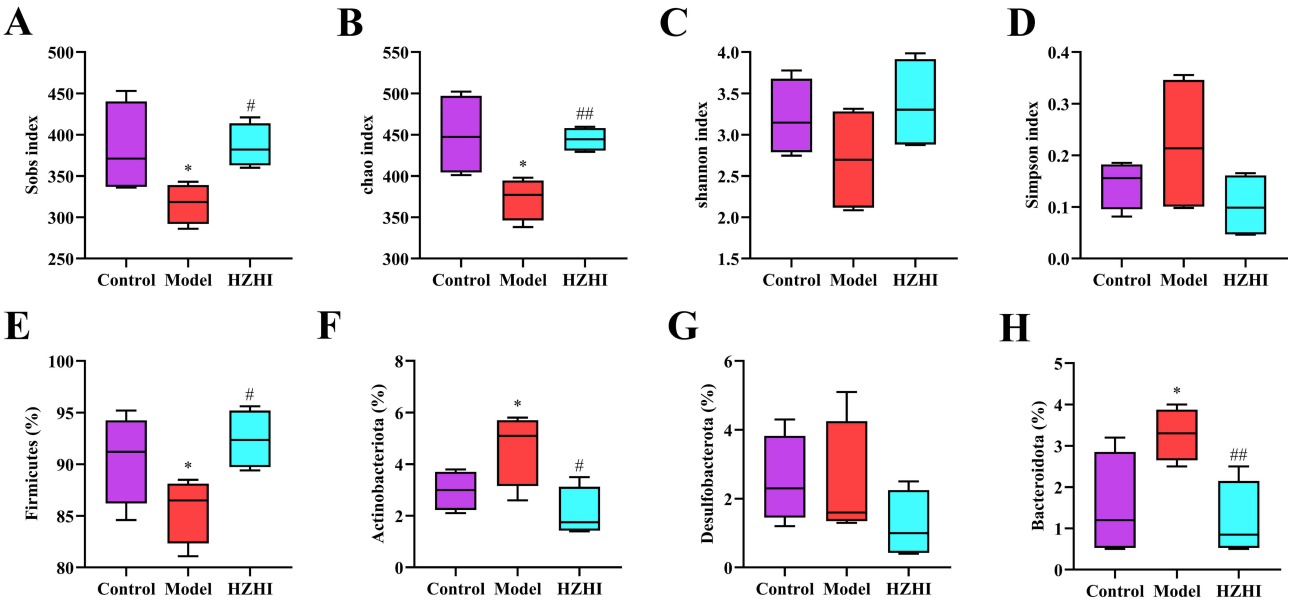

Figure 7 The influence of *T. chebula* on the structure of intestinal flora in HUA rats. (**A**) Sob index. (**B**) Chao index. (**C**) Shannon index. (**D**) Simpson index. (**E**) The relative abundance of *Firmicutes*. (**F**) The relative abundance of *Actinobacteriota*. (**G**) The relative abundance of *Desulfobacterota*. (**H**) The relative abundance of *Bacteroidota*. Values are presented as mean ± SD (n = 4 per group). Statistical significance was assessed using one-way ANOVA followed by Tukey's HSD test. $^{*}P< 0.05$ Control group; $^{\#}P < 0.05$, $^{\#\#}P < 0.05$ vs Model group.

drugs that not only reduce uric acid levels but also address other pathological aspects of HUA. The gut-kidney axis has emerged as a critical regulatory mechanism in uric acid metabolism, linking gut microbiota, intestinal barrier integrity, and renal function in a bidirectional relationship. Approximately two-thirds of uric acid is excreted by the kidneys, while the remaining one-third is cleared via the intestines. Impairments in either organ can exacerbate HUA pathology, with disruptions in intestinal homeostasis contributing to systemic inflammation and increased renal burden. This interconnection highlights the importance of therapies that target both gut and kidney health.

In this context, we identified *T. chebula* as a potential anti-HUA medicine through data mining and experimental validation. Compared to conventional therapies, *T. chebula* offers a broader therapeutic scope. While medications such as allopurinol primarily target uric acid reduction through xanthine oxidase (XOD) inhibition, *T. chebula* demonstrated additional benefits, including renal protection, improved intestinal barrier integrity, and modulation of gut microbiota. These multifaceted effects align with the gut-kidney axis framework, addressing key aspects of HUA pathology that are not effectively targeted by existing drugs. By modulating the gut microbiota, enhancing tight junction protein expression (eg, ZO-1, Occludin, and Claudin-1), and alleviating renal inflammation, *T. chebula* restores balance in the gut-kidney axis, highlighting its potential as a safer and more holistic treatment option.

Huang Shui is considered synonymous with HUA in Tibetan medicine.[13] Therefore, Huang Shui was chosen as the primary keyword for searching classical Tibetan medical texts and gathering relevant prescriptions. In the frequency analysis, the top 20 high-frequency herbs included *T. chebula*, Juemingzi, Ruxiang, Shexiang, Muxiang, Doukou, Huangkuizi, Maohezi, Shuichangpu, and Yuganzi, most of which were known to lower uric acid levels.[14–17] For example, Yuganzi extract demonstrated protective effects against acute gouty arthritis by reducing uric acid levels, inhibiting inflammation, and decreasing expression of MMP13.[18] Shuichangpu ethanolic extract reduced serum uric acid, calcium, phosphate, blood urea nitrogen, and creatinine levels in a urolithiatic rat model. Our analysis of Tibetan prescriptions used to treat HUA identified *T. chebula* as the Tibetan medicine with the highest frequency of occurrence. Surprisingly, there is currently no literature available on the uric acid-lowering effects of *T. chebula*.

The fruits of *Terminalia chebula Retz*., commonly referred to as "Hezi" in Chinese, belong to the "medicine food homology" plant and occupy a significant place in traditional Tibetan medicine.[19] Its usage is not limited to Tibet but extends to Southeast Asia and South Asia. *T. chebula* has various attributes in traditional medicine, including alterative, astringent, carminative, purgative, and stomachic properties.[20] *T. chebula* is well documented for its richness in phenolic

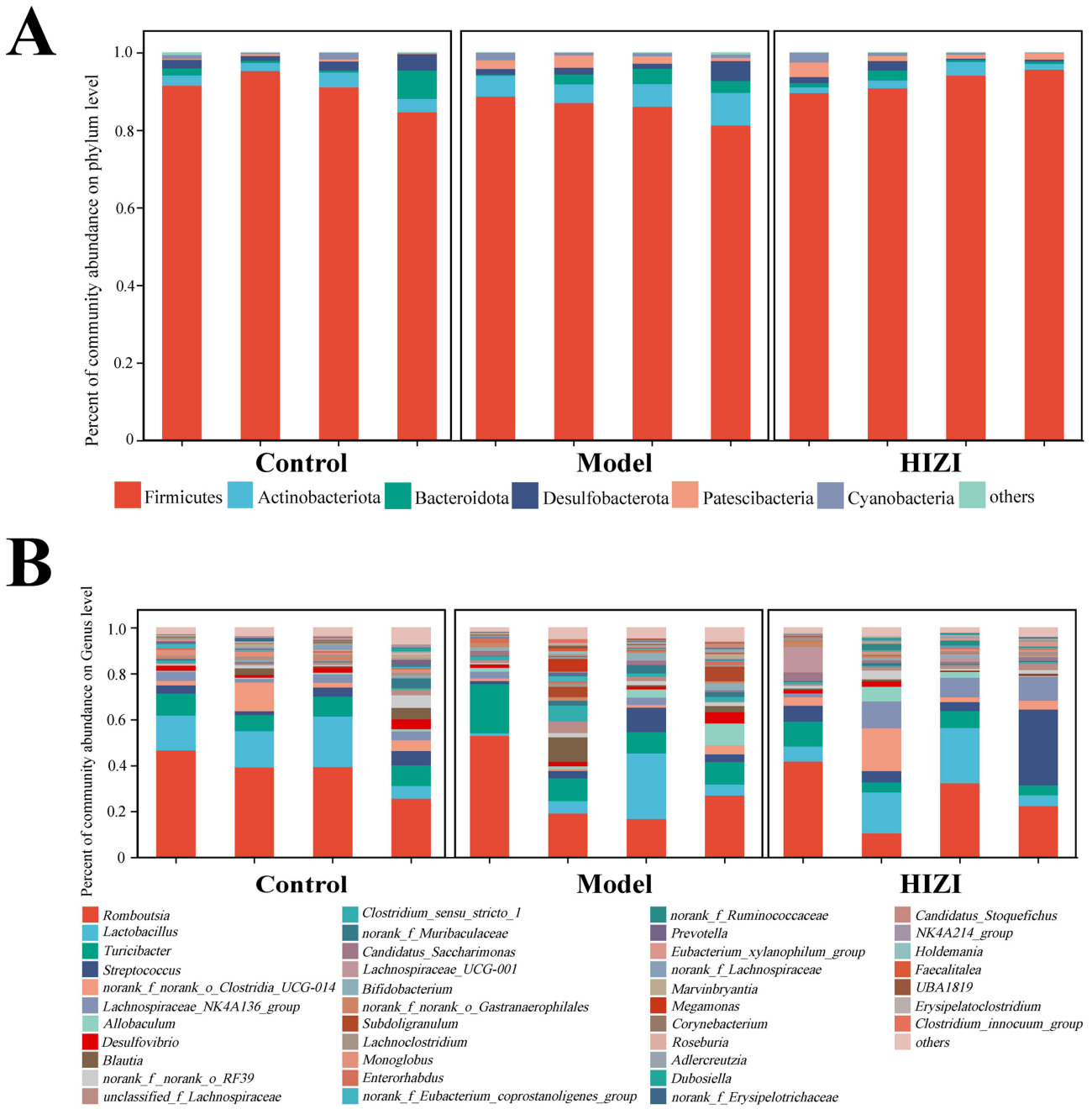

Figure 8 The influence of *T. chebula* on the species composition of intestinal flora in HUA rats at both the genus and phylum levels. (**A**) Percent of community abundance on Phylum level. (**B**) Percent of community abundance on Genus level. Values are presented as mean ± SD (n = 4 per group). Statistical significance was assessed using one-way ANOVA followed by Tukey's HSD test.

compounds such as gallic acid, ellagic acid, hydroxycinnamic acids, and their derivatives; tannins, including terflavin A, terchebulin, punicalagin, chebulagic acid, chebulinic acid, corilagin, and others; and flavonoids such as rutin, quercetin, and methylated derivatives of quercetin.[21] Existing literature has outlined the various pharmacological actions of *T. chebula*, including its neuroprotective effect,[22] anti-atopic dermatitis activity,[19] antimicrobial properties, anti-joint inflammatory potential,[23] and anti-tumor effects.[24] Importantly, this plant does not appear to induce debilitating or toxic side-effects.[15] In the context of Chinese medicine, *T. chebula* has been found in several prescriptions aimed at addressing hyperuricosis, including formulations such as Ershi WuWei LvXue, Wuwei SheXiang,[25] ShiWei RuXiang, ShiWuWei

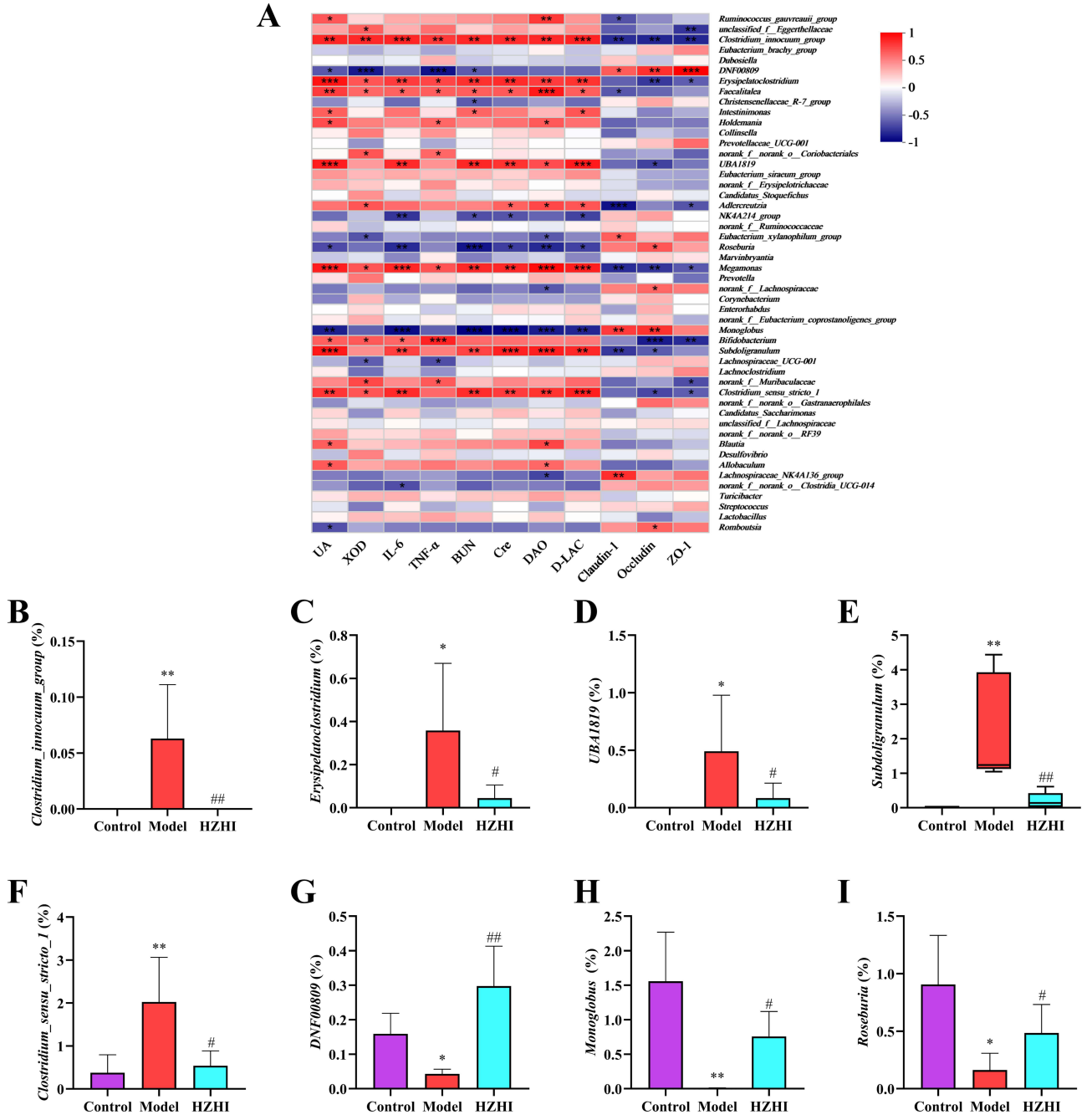

Figure 9 Changes of key gut microbiota among groups. (**A**) Spearman correlation analysis between intestinal flora and HUA index. (**B**) The relative abundance of *Clostridium_innocuum_group*. (**C**) The relative abundance of *Erysipelatoclostridium*. (**D**) The relative abundance of *UBA1819*. (**E**) The relative abundance of *Subdoligranulum*. (**F**) The relative abundance of *Clostridium_sensu_stricto_1*. (**G**) The relative abundance of *DNF00809*. (**H**) The relative abundance of *Monoglobus*. (**I**) The relative abundance of *Roseburia*. Values are presented as mean ± SD (n = 4 per group). Statistical significance was assessed using one-way ANOVA followed by Tukey's HSD test. **P*< 0.05, ***P*< 0.05 vs Control group; $^{\#}P < 0.05$, $^{\#\#}P < 0.05$ vs Model group.

RuPengSan,[8] and TongFeng TangSan. However, it is noteworthy that there are no reported instances of *T. chebula* being used for the treatment of HUA.

In this study, we initially assessed the in vitro inhibitory activity of *T. chebula* on XOD, and the results demonstrated dose-dependent inhibition of XOD by *T. chebula*. Subsequently, we established a HUA rat model using fructose and potassium oxonate to investigate the uric acid-lowering effects of *T. chebula* in vivo. Our findings not only confirmed a significant reduction in uric acid levels following *T. chebula* supplementation but also highlighted its role in restoring

gut-kidney axis balance. *T. chebula* ameliorated renal inflammation by reducing systemic levels of pro-inflammatory cytokines such as IL-6 and TNF-α, likely through the modulation of gut microbiota and the enhancement of intestinal barrier function. These improvements reduce endotoxin translocation, alleviating systemic inflammation and mitigating renal burden.

The kidneys are the primary organs responsible for uric acid excretion, and approximately two-thirds of uric acid is excreted through them.[26] HUA progression is often accompanied by renal injury. Elevated UA concentrations can increase renal burden, cause serious renal damage, and even cause chronic kidney disease. Cre and BUN levels are common clinical indicators of renal function, and their elevation often reflects severe renal insufficiency and various other kidney diseases.[27] Our research showed that HUA rats experienced serious renal damage, as reflected by significant increases in Cre and BUN levels. The decrease in serum BUN and Cre levels after *T. chebula* administration in the HUA group prompted *T. chebula* to effectively alleviate the kidney lesions. These results were confirmed by renal histopathological examination. Collectively, these results suggest that *T. chebula* supplementation can effectively alleviate renal dysfunction in HUA rats.

The intestine is an important organ for UA excretion, and approximately one-third of the circulating UA is cleared by intestinal enterocytes. UA excretion depends on intestinal homeostasis that is maintained by the intestinal mucosal barrier.[28] Serum DAO, D-Lac, and LPS levels are markers of intestinal permeability. DAO is an intracellular enzyme in the intestinal epithelium, whereas D-LAC and LPS are bacterial metabolites produced by intestinal flora.[29] Elevated serum levels of DAO, D-Lac, and LPS indicate increased intestinal permeability. After *T. chebula* intervention, the levels were significantly reduced. The apical junctional complex, a structure that holds intestinal cells together, is essential for maintaining the barrier that prevents harmful substances from entering the bloodstream. Claudin-1, Occludin, and ZO-1 are primary tight junction proteins. In the present study, immunohistochemistry and Q-PCR results showed that *T. chebula* supplementation significantly increased the reduced protein expression of claudin-1, occludin, and ZO-1 induced by HUA. These results indicate that administration of *T. chebula* contributes to the restoration of the intestinal barrier in HUA rats.

Furthermore, disruption of intestinal barrier integrity can lead to the translocation of bacteria or bacterial products, such as lipopolysaccharide (LPS), into the bloodstream, triggering the innate immune system and causing chronic systemic inflammation and metabolic disorders.[30] In the model group, serum levels of inflammatory cytokines (IL-6, IL-1β, and TNF-α) were significantly higher than those in the control group, confirming the presence of systemic low-grade inflammation. Furthermore, studies have shown that chronic inflammation induced by elevated serum LPS levels is often accompanied by increased XOD activity.[31] Administration of *T. chebula* effectively alleviated inflammatory reactions and XOD activity in rats with HUA.

Numerous studies have shown that intestinal flora is an important factor related to HUA.[32–34] According to current research, the effect of intestinal flora on HUA is mainly achieved in three ways: participation in purine metabolism, decomposition of uric acid, and reduction of uric acid levels.[35] Metabolites produced by intestinal flora promote the excretion of uric acid, repair the intestinal barrier, and reducing inflammation associated with HUA.[34] In our study, *T. chebula* treatment significantly changed the composition and structure of intestinal flora in HUA rats. Consistent with previous studies,[36–38] at the phylum level, rats in the model group showed a lower abundance of *Firmicutes* and an increased abundance of *Bacteroidetes* than rats in the control group. Intervention with *T. chebula* has the potential to reverse such variations in *Firmicutes* and *Bacteroidota*.

At the genus level, our correlation analysis revealed that several bacteria, including *Clostridium innocuum, Clostridium_sensu_stricto_1*, Erysipelatoclostridium, *Subdoligranulum, Megamonas, Faecalitalea*, and *UBA1819*, were risk factors for HUA, while Monoglobus, *DNF00809*, and *Roseburia* were protective factors. These findings are consistent with those of previous studies reporting similar results. For example, previous research has demonstrated a positive correlation between Clostridium spp. and uric acid levels.[39,40] *Erysipelatoclostridium*, a potential opportunistic pathogen, was enriched in patients with gout,[41] and its relative abundance increased after exposure to uric acid, whereas JL-3 treatment reduced its abundance.[29] Additionally, Liu et al found that *Subdoligranulum* was more abundant in the intestinal tract of rats with high purine-induced HUA than in normal rats.[42] In contrast, our study also observed variations in UBA1819 levels, as end-stage diabetic kidney patients exhibited a higher abundance of this bacterium, which was inversely correlated with UA levels.[43] Our results demonstrate that *T. chebula* can effectively reduce the levels of these harmful bacteria, including *Clostridium_innocuum_group, Erysipelatoclostridium, UBA1819, Subdoligranulum*, and *Clostridium_sensu_stricto_1*. Additionally, an in vitro study showed that *T. chebula* extract displayed strong inhibitory activity against *Clostridium perfringens* with no adverse effects on the growth of several probiotics.[44]

One major limitation of this study is the reduced sample size (n = 4) for microbiota analysis, which limits the statistical power and generalizability of the findings. This small sample size was due to sample contamination and logistical constraints during the experimental process. While the results are consistent with previous literature on hyperuricemia-related gut microbiota changes, they should be interpreted as exploratory. Future studies with larger cohorts are essential to confirm the observed microbial shifts and establish stronger statistical significance.

In addition, *T. chebula* significantly increased the levels of certain beneficial bacteria including *Monoglobus, DNF00809*, and *Roseburia*. It has been reported that both *Monoglobus* and *Roseburia* possess the ability to ferment dietary fiber, facilitating butyrate production.[45,46] Butyrate can enhance intestinal barrier function by inducing the expression of tight junction proteins such as ZO-1 and Occludin.[47] In our study, the increased expression of ZO-1 and Occludin was attributed to the increased production of butyrate. *Roseburia*-derived butyrate has been shown to suppress gout flares by reducing the production of IL-1β, IL-6, and IL-8 induced by monosodium urate (MSU) crystals.[48] Furthermore, *Roseburia* is associated with improved renal function.[49] These findings provide valuable insights into the potential of *T. chebula* treatment to induce HUA remission by affecting the composition of gut microbiota. However, further research is needed to fully understand the mechanism by which *T. chebula* regulates the gut microbiota.

While our study highlights potential gut microbiota changes linked to *T. chebula* treatment, the limited sample size weakens the statistical robustness of these findings. As such, these results provide a foundation for future research rather than definitive conclusions about the relationship between microbiota modulation and HUA treatment. To address the limitations of this study, future research should involve larger cohorts to increase statistical power and confirm the observed microbial shifts. Additionally, integrating functional metagenomics or metabolomics could provide deeper mechanistic insights into how specific microbial changes mediate the therapeutic effects of *T. chebula*.

Conclusion

In conclusion, our study revealed that *T. chebula* is a promising therapeutic agent for HUA treatment based on the rich heritage of traditional Tibetan medicine. Using data mining and experimental validation, we found that *T. chebula* extract demonstrated efficacy in reducing serum uric acid levels, mitigating renal injury, enhancing intestinal barrier function, and modulating gut microbiota composition in a HUA rat model. These findings highlight *T. chebula* as a safe and effective herb for the management of HUA. Furthermore, our research underscores the value of traditional Tibetan medicine in addressing metabolic disorders, and offers a promising avenue for developing alternative treatments for HUA and related conditions.

Data Sharing Statement

The raw data supporting the conclusions of this study are made available by the authors upon request.

Ethics Statement

The animal research involved in this study was approved by the Animal Ethics Committee of Guangdong Pharmaceutical University (permit number: SPF2017660). All animal experiments were performed in compliance with the Guidelines for Ethical Review of Laboratory Animal Welfare (GB/T 35892-2018) issued by the Standardization Administration of China.

Acknowledgments

We would like to express our sincere appreciation to the reviewers for their critical comments regarding this article.

Author Contributions

All authors made a significant contribution to the work reported, whether in the conception, study design, execution, acquisition of data, analysis, and interpretation, or in all these areas; took part in drafting, revising, or critically reviewing the article; gave final approval of the version to be published; have agreed on the journal to which the article has been submitted; and agree to be accountable for all aspects of the work.

Funding

This work was funded by the Guangzhou Science and Technology Planning Project (202201010357), Project of Administration of Traditional Chinese Medicine Guangdong Province (20232086), and the Guangdong Medical Science and Technology Research Foundation (A2022069).

Disclosure

The authors report no conflicts of interest in this work.

References

1. Zhang M, Zhu X, Wu J, et al. Prevalence of hyperuricemia among Chinese adults: findings from two nationally representative cross-sectional surveys in 2015–16 and 2018–19. *Front Immunol*. 2022;12:791983. doi:10.3389/fimmu.2021.791983
2. Petreski T, Ekart R, Hojs R, Hyperuricemia BS. the heart, and the kidneys - to treat or not to treat? *Ren Fail*. 2020;42(1):978–986. doi:10.1080/0886022X.2020.1822185
3. Amatjan M, Li N, He P, et al. A novel approach based on gut microbiota analysis and network pharmacology to explain the mechanisms of action of Cichorium intybus L. Formula in the improvement of hyperuricemic nephropathy in rats. *Drug Des Devel Ther*. 2023;17:107–128. doi:10.2147/DDDT.S389811
4. Gao Y, Sun J, Zhang Y, et al. Effect of a traditional Chinese medicine formula (CoTOL) on serum uric acid and intestinal flora in obese hyperuricemic mice inoculated with intestinal bacteria. *Evidence-Based Complem Alter Med*. 2020;2020(1):8831937. doi:10.1155/2020/8831937
5. Zhang Q, Gong H, Lin C, et al. The prevalence of gout and hyperuricemia in middle-aged and elderly people in Tibet Autonomous Region, China. *Medicine*. 2020;99(2):e18542. doi:10.1097/MD.0000000000018542
6. El-Tantawy WH. Natural products for the management of hyperuricaemia and gout: a review. *Arch Physiol Biochem*. 2021;127(1):61–72. doi:10.1080/13813455.2019.1610779
7. Li Q, Liu P, Wu C, et al. Integrating network pharmacology and pharmacological validation to explore the effect of Shi Wei Ru Xiang powder on suppressing hyperuricemia. *J Ethnopharmacol*. 2022;298:115679. doi:10.1016/j.jep.2022.115679
8. fang CH, Zhang C, Yao Y, et al. Study on anti-hyperuricemia effects and active ingredients of traditional Tibetan medicine TongFengTangSan (TFTS) by ultra-high-performance liquid chromatography coupled with quadrupole time-of-flight mass spectrometry. *J Pharm Biomed Anal*. 2019;165:213–223. doi:10.1016/j.jpba.2018.11.038
9. Huang Z, Zhang W, An Q, et al. Exploration of the anti-hyperuricemia effect of TongFengTangSan (TFTS) by UPLC-Q-TOF/MS-based non-targeted metabonomics. *Chin Med*. 2023;18(1):17. doi:10.1186/s13020-023-00716-w
10. Wang X, Zhang X, Li J, et al. Analysis of prescription medication rules of traditional Chinese medicine for bradyarrhythmia treatment based on data mining. *Medicine*. 2022;101(44):e31436. doi:10.1097/MD.0000000000031436
11. Yang B, Xin M, Liang S, et al. Naringenin ameliorates hyperuricemia by regulating renal uric acid excretion via the PI3K/AKT signaling pathway and renal inflammation through the NF-κB signaling pathway. *J Agric Food Chem*. 2023;71(3):1434–1446. doi:10.1021/acs.jafc.2c01513
12. Chen-Xu M, Yokose C, Rai SK, Pillinger MH, Choi HK. Contemporary prevalence of gout and hyperuricemia in the United States and decadal trends: the national health and nutrition examination survey, 2007–2016. *Arthritis Rheumatol*. 2019;71(6):991–999. doi:10.1002/art.40807
13. Yong Zong ZW, Si Lang JY, De L, jia GZ, Zhang Y. Study the compositional principle of gout in Tibetan medicine on the data technology. *Lishizhen Med Materia Medica Res*. 2017;28(12):3035–3036.
14. Yiying K, Yongfang L, Husai M, Wangyu L, Ruilian L, Zhancui D. Uric acid lowering effect of Tibetan Medicine RuPeng15 powder in animal models of hyperuricemia. *J Trad Chinese Med*. 2016;36(2):205–210. doi:10.1016/S0254-6272(16)30028-0
15. Ekambaram SP, Babu KB, Perumal SS, Rajendran D. Repeated oral dose toxicity study on hydrolysable tannin rich fraction isolated from fruit pericarps of Terminalia chebula Retz in Wistar albino rats. *Regul Toxicol Pharmacol*. 2018;92:182–188. doi:10.1016/j.yrtph.2017.12.001
16. Lang J, Li L, Chen S, et al. Mechanism Investigation of Wuwei Shexiang pills on gouty arthritis via network pharmacology, molecule docking, and pharmacological verification. *Evidence-Based Complem Alter Med*. 2022;2022:1–19. doi:10.1155/2022/2377692
17. Yu XN, Wu HY, Deng YP, et al. "Yellow-dragon wonderful-seed formula" for hyperuricemia in gout patients with dampness-heat pouring downward pattern: a pilot randomized controlled trial. *Trials*. 2018;19(1):551. doi:10.1186/s13063-018-2917-8
18. Tao H, Zhong J, Mo Y, Liu W, Wang H. Exploring the mechanism through which Phyllanthus emblica L. Extract exerts protective effects against acute gouty arthritis: a network pharmacology study and experimental validation. *Evidence-Based Complem Alter Med*. 2022;2022:1–16. doi:10.1155/2022/9748338
19. Kim HJ, Song HK, Park SH, et al. Terminalia chebula Retz. extract ameliorates the symptoms of atopic dermatitis by regulating anti-inflammatory factors in vivo and suppressing STAT1/3 and NF-κB signaling in vitro. *Phytomedicine*. 2022;104:154318. doi:10.1016/j.phymed.2022.154318
20. Bulbul MdR H, Uddin Chowdhury MN, Naima TA, et al. A comprehensive review on the diverse pharmacological perspectives of Terminalia chebula Retz. *Heliyon*. 2022;8(8):e10220. doi:10.1016/j.heliyon.2022.e10220
21. Nigam M, Mishra AP, Adhikari-Devkota A, et al. Fruits of *Terminalia chebula*Retz.: a review on traditional uses, bioactive chemical constituents and pharmacological activities. *Phytother Res*. 2020;34(10):2518–2533. doi:10.1002/ptr.6702
22. Zhao L, Duan Z, Wang Y, et al. Protective effect of Terminalia chebula Retz. extract against Aβ aggregation and Aβ-induced toxicity in Caenorhabditis elegans. *J Ethnopharmacol*. 2021;268:113640. doi:10.1016/j.jep.2020.113640
23. Ekambaram SP, Perumal SS, Erusappan T, Srinivasan A. Hydrolysable tannin-rich fraction from Terminalia chebula Retz. fruits ameliorates collagen-induced arthritis in BALB/c mice. *Inflammopharmacology*. 2020;28(1):275–287. doi:10.1007/s10787-019-00629-x
24. Mehrabani M, Jafarinejad-Farsangi S, Raeiszadeh M, et al. Effects of the ethanol and ethyl acetate extracts of Terminalia chebula Retz. on proliferation, migration, and HIF-1α and CXCR-4 expression in MCF-7 cells: an in vitro study. *Appl Biochem Biotechnol*. 2023;195(5):3327–3344. doi:10.1007/s12010-022-04301-z

25. Bai L, Wu C, Lei S, et al. Potential anti-gout properties of Wuwei Shexiang pills based on network pharmacology and pharmacological verification. *J Ethnopharmacol*. 2023;305:116147. doi:10.1016/j.jep.2023.116147
26. Copur S, Demiray A, Kanbay M. Uric acid in metabolic syndrome: does uric acid have a definitive role? *Eur J Intern Med*. 2022;103:4–12. doi:10.1016/j.ejim.2022.04.022
27. Pan B, Zhang H, Hong Y, Ma M, Wan X, Cao C. Indoleamine-2,3-Dioxygenase Activates Wnt/β-Catenin Inducing Kidney Fibrosis after Acute Kidney Injury. *Gerontology*. 2021;67(5):611–619. doi:10.1159/000515041
28. Guo Y, Li H, Liu Z, et al. Impaired intestinal barrier function in a mouse model of hyperuricemia. *Mol Med Rep*. 2019;20(4):3292–3300. doi:10.3892/mmr.2019.10586
29. Wu Y, Ye Z, Feng P, et al. Limosilactobacillus fermentum JL-3 isolated from "Jiangshui" ameliorates hyperuricemia by degrading uric acid. *Gut Microbes*. 2021;13(1):1897211. doi:10.1080/19490976.2021.1897211
30. Xu D, Lv Q, Wang X, et al. Hyperuricemia is associated with impaired intestinal permeability in mice. *Ame J Physiol-Gastrointestinal Liver Physiol*. 2019;317(4):G484–G492. doi:10.1152/ajpgi.00151.2019
31. Ramos MF de P, Monteiro de Barros A Do CM, Razvickas CV, Borges FT, Schor N. Xanthine oxidase inhibitors and sepsis. *Int J Immunopathol Pharmacol*. 2018;32:2058738418772210. doi:10.1177/2058738418772210
32. Wang J, Chen Y, Zhong H, et al. The gut microbiota as a target to control hyperuricemia pathogenesis: potential mechanisms and therapeutic strategies. *Crit Rev Food Sci Nutr*. 2022;62(14):3979–3989. doi:10.1080/10408398.2021.1874287
33. Wang Z, Li Y, Liao W, et al. Gut microbiota remodeling: a promising therapeutic strategy to confront hyperuricemia and gout. *Front Cell Infect Microbiol*. 2022;12:935723. doi:10.3389/fcimb.2022.935723
34. Yin H, Liu N, Chen J. The Role of the Intestine in the Development of Hyperuricemia. *Front Immunol*. 2022;13:845684. doi:10.3389/fimmu.2022.845684
35. Liu Y, Jarman JB, Low YS, et al. A widely distributed gene cluster compensates for uricase loss in hominids. *Cell*. 2023;186(16):3400–3413.e20. doi:10.1016/j.cell.2023.06.010
36. Wang R, Halimulati M, Huang X, Ma Y, Li L, Zhang Z. Sulforaphane-driven reprogramming of gut microbiome and metabolome ameliorates the progression of hyperuricemia. *J Adv Res*. 2023;52:19–28. doi:10.1016/j.jare.2022.11.003
37. Chen Y, Pei C, Chen Y, et al. Kidney tea ameliorates hyperuricemia in mice via altering gut microbiota and restoring metabolic profile. *Chem Biol Interact*. 2023;376:110449. doi:10.1016/j.cbi.2023.110449
38. Fan S, Huang Y, Lu G, et al. Novel anti-hyperuricemic hexapeptides derived from *Apostichopus japonicus* hydrolysate and their modulation effects on the gut microbiota and host microRNA profile. *Food Funct*. 2022;13(7):3865–3878. doi:10.1039/D1FO03981D
39. Zeng Q, Li D, He Y, et al. Discrepant gut microbiota markers for the classification of obesity-related metabolic abnormalities. *Sci Rep*. 2019;9(1):13424. doi:10.1038/s41598-019-49462-w
40. Rafiq T, Stearns JC, Shanmuganathan M, et al. Integrative multiomics analysis of infant gut microbiome and serum metabolome reveals key molecular biomarkers of early onset childhood obesity. *Heliyon*. 2023;9(6):e16651. doi:10.1016/j.heliyon.2023.e16651
41. He S, Xiong Q, Tian C, et al. Inulin-type prebiotics reduce serum uric acid levels via gut microbiota modulation: a randomized, controlled crossover trial in peritoneal dialysis patients. *Eur J Nutr*. 2022;61(2):665–677. doi:10.1007/s00394-021-02669-y
42. Liu X, Lv Q, Ren H, et al. The altered gut microbiota of high-purine-induced hyperuricemia rats and its correlation with hyperuricemia. *Peer J*. 2020;8(3):e8664. doi:10.7717/peerj.8664
43. Chen R, Zhu D, Yang R, et al. Gut microbiota diversity in middle-aged and elderly patients with end-stage diabetic kidney disease. *Ann Transl Med*. 2022;10(13). doi:10.21037/atm-22-2926
44. Kim HG, Cho JH, Jeong EY, Lim JH, Lee SH, Lee HS. Growth-inhibiting activity of active component isolated from Terminalia chebula fruits against intestinal bacteria. *J Food Prot*. 2006;69(9):2205–2209. doi:10.4315/0362-028X-69.9.2205
45. de MVN, Gomes MJC, Grancieri M, et al. Chia (Salvia hispanica L.) flour modulates the intestinal microbiota in Wistar rats fed a high-fat and high-fructose diet. *Food Res Int*. 2023;172:113095. doi:10.1016/j.foodres.2023.113095
46. Hao Y, Ji Z, Shen Z, et al. Increase dietary fiber intake ameliorates cecal morphology and drives cecal species-specific of short-chain fatty acids in white Pekin ducks. *Front Microbiol*. 2022;13:853797. doi:10.3389/fmicb.2022.853797
47. Salvi PS, Cowles RA. Butyrate and the intestinal epithelium: modulation of proliferation and inflammation in homeostasis and disease. *Cells*. 2021;10(7):1775. doi:10.3390/cells10071775
48. Martínez-Nava GA, Méndez-Salazar EO, Vázquez-Mellado J, et al. The impact of short-chain fatty acid–producing bacteria of the gut microbiota in hyperuricemia and gout diagnosis. *Clin Rheumatol*. 2023;42(1):203–214. doi:10.1007/s10067-022-06392-9
49. Pan L, Han P, Ma S, et al. Abnormal metabolism of gut microbiota reveals the possible molecular mechanism of nephropathy induced by hyperuricemia. *Acta Pharm Sin B*. 2020;10(2):249–261. doi:10.1016/j.apsb.2019.10.007